Hyperbaric oxygen ameliorates bleomycin-induced pulmonary fibrosis in mice

Yuan Yuan[1†], Yali Li[1†], Guoqiang Qiao[1], Yilu Zhou[2,3], Zijian Xu[2], Charlotte Hill[2], Zhenglin Jiang[1*], Yihua Wang[2,3*]

[1]Department of Neurophysiology and Neuropharmacology, Institute of Special Environmental Medicine and Co-innovation Center of Neuroregeneration, Nantong University, Nantong, Jiangsu, China;

[2]Biological Sciences, Faculty of Environmental and Life Sciences, University of Southampton, Southampton SO17 1BJ, UK.

[3]Institute for Life Sciences, University of Southampton, Southampton SO17 1BJ, UK.

[†]These authors contributed equally and share the first authorship.

***Correspondence:**
Yihua Wang
yihua.wang@soton.ac.uk

Zhenglin Jiang
jiangzl@ntu.edu.cn

Keywords: Pulmonary fibrosis, Hyperbaric oxygen, Fibroblast, differentiation, Extracellular matrix.

Word count: 3201

Figure number: 6 in the main text, and 5 in the supplementary material

Abstract

The prevalence of pulmonary fibrosis is increasing with an ageing population and its burden is likely to increase following COVID-19, with large financial and medical implications. As approved therapies in pulmonary fibrosis only slow disease progression there is a significant unmet medical need. Hyperbaric oxygen (HBO) is the inhaling of pure oxygen, under the pressure of greater than one atmosphere absolute and it has been reported to improve pulmonary function in patients with pulmonary fibrosis. Our recent study suggested that repetitive HBO exposure may affect biological processes in mice lungs such as response to wounding and extracellular matrix. To extend these findings, a bleomycin-induced pulmonary fibrosis mouse model was used to evaluate the effect of repetitive HBO exposure on pulmonary fibrosis. Building on our previous findings, we provide evidence that HBO exposure attenuates bleomycin-induced pulmonary fibrosis in mice. *In vitro*, HBO exposure could reverse, at least partially, transforming growth factor (TGF)-β-induced fibroblast activation, and this effect may be mediated by down-regulating TGF-β-induced expression of hypoxia inducible factor (HIF)-1α. These findings support HBO as a potentially life-changing therapy for patients with pulmonary fibrosis, although further research is needed to fully evaluate this.

Introduction

Pulmonary fibrosis, an interstitial lung disease, is characterised by enhanced deposition and remodeling of the extracellular matrix (ECM), leading to disrupted gas-exchange, and ultimately respiratory failure and death (Richeldi et al., 2017). The prevalence of pulmonary fibrosis is increasing with an ageing population (Richeldi et al., 2017) and its burden after COVID-19 recovery could be substantial (George et al., 2020). Idiopathic pulmonary fibrosis (IPF), the most common type of progressive fibrotic interstitial lung disease, affects 5 million people worldwide (Meltzer and Noble, 2008), with a median survival of 3 years (Goodwin and Jenkins, 2016; Richeldi et al., 2017). The current approved therapies for pulmonary fibrosis only slow the disease progression, and as such there is a demand for new treatment options.

Current clinical management of IPF patients includes anti-fibrotic drugs and non-pharmacological support (Richeldi et al., 2017). For patients with advanced disease, reducing symptoms and improving quality of life are required (Zou et al., 2020). Long-term oxygen therapy, with high flow and high concentration of oxygen, is often used to decrease dyspnea and improve exercise tolerance (Koyauchi et al., 2018; Faverio et al., 2019). It is also reported that oxygen supplementation increased exercise capacity for patients with interstitial lung diseases including IPF (Bell et al., 2017; Dowman et al., 2017). Moreover, the benefit of high flow oxygen compared to placebo air was found to improve the quality of life for patients with fibrotic lung disease in a clinical trial (Visca et al., 2018).

Hyperbaric oxygen (HBO) involves inhaling pure oxygen in a closed chamber pressurised to greater than 1 atmosphere absolute (ATA). The clinical applications of HBO in ischemic and nonhealing wounds have been reported since the mid-20th century (Lam et al., 2017). An updated list of its applications can be found on the Undersea and Hyperbaric Medical Society website (https://www.uhms.org/resources/hbo-indications.html), and have also been reviewed elsewhere (Choudhury, 2018; Kirby, 2019). Interestingly, HBO therapy has been reported to improve pulmonary function in IPF patients (Ma and Du, 2003; Qiu et al., 2013). In another report, HBO exposure reduced radiation-induced side effects including fibrosis in a rat bladder irradiation model (Oscarsson et al., 2017). Mechanistically, our recent study suggested that repetitive HBO exposure may affect biological processes in mice lungs such as response to wounding and ECM (Yuan et al., 2020). To extend these findings, a bleomycin-induced pulmonary fibrosis mouse model was used to evaluate the effect of repetitive HBO exposure on pulmonary fibrosis. Building on our previous report (Yuan et al., 2020), we provide evidence that HBO exposure attenuates bleomycin-induced pulmonary fibrosis in mice. *In vitro*, HBO exposure could reverse, at least partially, transforming growth factor (TGF)-β-induced fibroblast activation. These findings support HBO as a potentially life-changing therapy for patients with pulmonary fibrosis, although further research is needed to fully evaluate its benefit to see if the benefits outweigh the risks.

Materials and Methods

Pathway enrichment analysis

The RNA-seq data analysed were based on our previous study (Yuan et al., 2020) (GSE143348). Briefly, lungs were collected from control mice or HBO-treated mice that were repetitively exposed to 2.5 ATA HBO, 90 min/time, once a day for 11 consecutive days. Control mice were placed in the chamber for the same duration without pure oxygen pressurization. Lung samples were collected on the next day of the last HBO exposure. Total RNA was isolated for library construction, and was sequenced with paired-end strategy (2 ×150) on the Illumina NovaSeq 6000 platform following the standard protocols. Enrichment analyses of down-regulated differentially expressed genes (DEGs) were generated by Metascape with default parameters (https://metascape.org/gp/index.html#/main/step1). All significantly enriched gene ontology (GO) terms and their *P* values were imported into REVIGO (http://revigo.irb.hr/) to remove redundant GO terms. GO: 0062023 (collagen containing extracellular matrix) and GO: 0031012 (extracellular matrix) gene lists were downloaded from MSigDB Collections (http://www.gsea-msigdb.org/gsea/msigdb/) and converted into corresponding mouse genes. Based on these gene lists, the pathway enrichment score for each sample was calculated by using gene set variation analysis in the GSVA (v 1.36.2) package (Hanzelmann et al., 2013).

Bleomycin-induced pulmonary fibrosis in mice

Six to eight week old male C57BL/6 mice were purchased from the Experimental Animal Center of Nantong University (institutional license: SYXK(SU)-2012-0030). Mice were maintained under a 12-hour light/12-hour dark cycle, normal diet and water were provided *ad libitum* throughout the study. Animal experiments were approved by the Animal Ethics Committee at Nantong University (approval number: 20140901-001).

One dose of 2.0 U/kg of bleomycin (Hisun Pfizer Pharmaceutical Co., Ltd, Zhejiang, China) was intratracheally instilled to induce pulmonary fibrosis in mice. After bleomycin administration, body weights were monitored every third day. According to the previous report, weight loss is an indicator of successful model construction (Vandivort et al., 2016), mice with a weight loss of less than 5% at day 7 or less than 10% at day 10 post bleomycin challenge were excluded from further study.

HBO exposure of mice or cells

A hyperbaric chamber designed for small animal research was used for HBO exposure, as described previously (Yuan et al., 2020). Briefly, after the chamber was flushed with pure oxygen for 5 minutes, the pressure ramped up to 2.5 ATA (1.5 atm) by inflating 100% oxygen slowly in 5 minutes, then sustained at 2.5 ATA for 90 min, finally decompressed slowly in 5 minutes. The concentrations of carbon dioxide and oxygen were monitored by SDA carbon dioxide and oxygen monitors (ANALOX, North Yorkshire, England) during the exposure. Bleomycin-challenged mice were randomised into control or HBO-treated group, in which HBO exposure was applied daily from day 7 after intratracheal bleomycin instillation until day 20, and samples were collected at day 21. Mice in the control group were maintained in the normoxia condition throughout the study. Before sample collections, mice were anesthetized with composited anesthetics (257 mM chloral hydrate, 176 mM magnesium sulfate, 36 mM pentobarbital sodium, 14.25% ethanol, and 33.8% propylene glycol).

To treat cells with HBO, a hyperbaric chamber designed for cell culture was used. An embedded circulating water device was used to keep the environmental temperature at 37 °C. HBO exposure was applied at 2.5 ATA for 90 minutes. To maintain the pH of cell culture medium, the mixed gas with 98% oxygen and 2% carbon dioxide was used to maintain the partial pressure of carbon dioxide at 5 kPa under 2.5 ATA pressure.

Hematoxylin and eosin (H/E) and Masson's Trichrome staining

The left lung lobes of the mice were used for morphological examinations. Lungs were fixed with 4% paraformaldehyde for 24 hours, dehydrated by gradient ethanol, embedded in paraffin, and sliced 5 μm thick successively. For staining experiments, the tissue sections were de-waxed and rehydrated. For H/E staining, a H/E stain kit (Beyotime Biotechnology, Shanghai, China) was used according to the protocol. For Masson's trichrome stain, a Masson stain kit (Nanjing Jiancheng Bioengineering Institute, Jiangsu, China) was used following the manufacturer's instructions. DM4000B microscope (Leica, Wetzlar, Germany) was used for imaging.

Ashcroft score evaluation

Ashcroft scores were evaluated as previously described (Hubner et al., 2008). To ensure the accuracy of the results, a double-blind strategy was adopted when scoring. Two researchers were asked to score without knowing group information, and the means of the scores for each sample were used for further statistical analysis.

Hydroxyproline quantification

Lung tissues were harvested from mice at day 21 after bleomycin administration. Following excision, tissues were immediately flash frozen in liquid nitrogen. A hydroxyproline assay kit from KeyGEN BioTECH (Jiangsu, China) was used to detected hydroxyproline levels in lungs following the manufacturer's instructions. Hydroxyproline contents were normalized to the lung tissue mass.

Cell culture and reagents

Human lung fibroblast HFL1 cells were purchased from the Institute of Cell Research (Chinese Academy of Sciences) and were cultured in Nutrient Mixture F-12 Ham (Sigma-Aldrich, Massachusetts, USA) cell culture medium containing 10% fetal bovine serum (Gibco, New York, USA) and 1% penicillin/streptomycin. Cells were cultured in a 37°C incubator containing 5% CO_2. No *mycoplasma* contamination was detected in the cell line used. TGF-β was from PeproTech (New Jersey, USA).

Western blot analysis

Protein samples from cells or lung tissues were lysed with RIPA buffer (Beyotime Biotechnology, Shanghai, China) containing protease inhibitor (Meilunbio, Liaoning, China). Primary antibodies were from Cell Signaling Technology (α-SMA, 14968), Sigma-Aldrich (β-actin, A5316), and R&D Systems (HIF-1α, AF1935). Signals were detected using an ECL detection system with Tanon 5200 Multi imaging system (Shanghai, China), and evaluated by ImageJ 1.42q software (National Institutes of Health).

Real-time qPCR analysis

Total RNA samples were isolated from cultured cells or lung tissues with TRIzol reagent (Invitrogen, California, USA), following the manufacturer's instructions and quantified using a One Drop OD-1000+ Spectrophotometer (One Drop, Shanghai, China). HiScript II RT SuperMix for qPCR was used for reverse transcriptions (+ gDNA wiper) (Vazyme, Jiangsu, China). Universal SYBR qPCR Master Mix was used for qPCR assays (Vazyme, Jiangsu, China). Relative transcript levels of target genes were normalised to β-actin (*ACTB* in human and *Actb* in mouse). Primers for the genes detected were as following:

Human *ACTA2*-Forward: ACTGCCTTGGTGTGTGACAA,

Human *ACTA2*-Reverse: CACCATCACCCCCTGATGTC;

Human *FN1*-Forward: AGGAAGCCGAGGTTTTAACTG,
Human *FN1*-Reverse: AGGACGCTCATAAGTGTCACC;
Human *COL1A1*-Forward: GAGGGCCAAGACGAAGACATC,
Human *COL1A1*-Reverse: CAGATCACGTCATCGCACAAC;
Human *ACTB*-Forward: GGATTCCTATGTGGGCGACGA,
Human *ACTB*-Reverse: GCGTACAGGGATAGCACAGC;
Mouse *Acta2*-Forward: TCCCTGGAGAAGAGCTACGAAC,
Mouse *Acta2*-Reverse: AGGACGTTGTTAGCATAGAGATCC;
Mouse *Col1a1*-Forward: AGCACGTCTGGTTTGGAGAG,
Mouse *Col1a1*-Reverse: GACATTAGGCGCAGGAAGGT;
Mouse *Fn1*-Forward: CCCCAACTGGTTACCCTTCC,
Mouse *Fn1*-Reverse: TGTCCGCCTAAAGCCATGTT;
Mouse *Actb*-Forward: ACACCCGCCACCAGTTC,
Mouse *Actb*-Reverse: TACAGCCCGGGGAGCAT.

Statistical analysis and repeatability of experiments

Each experiment was repeated at least twice. Data are presented as mean and standard deviation (s.d.). A two tailed, unpaired, parametric or nonparametric t-test was used to compare two groups of values, depending on whether the data distribution passed the normality test. One outlier in Ashcroft scores identified by ROUT analysis (Q = 1%) was removed from statistical analysis. One-way ANOVA (single-factor analysis of variance) was used to compare more than two groups of data. Two-way ANOVA (two-factors analysis of variance) was applied to analyze the difference of body weight change curve. GraphPad Prism 8.0 software was used for analysis and $P < 0.05$ was considered as statistically significant.

Results

Repetitive HBO treatments down-regulates extracellular matrix gene expression in mouse lungs.

Our previous study suggested that repetitive HBO treaments may affect biological processes in the lungs, such as response to wounding and extracellular matrix (ECM) (Yuan et al., 2020). We reported that in the down-regulated genes in mice lungs following repetitive HBO exposure (GSE143348), enriched terms for cellular component classification included “collagen containing extracellular matrix” and “extracellular matrix component”, suggesting that the extracellular matrix may be affected (Yuan et al., 2020). These findings were also reflected using the REVIGO TreeMap, which found "extracellular matrix" as a GO enriched term (Fig. 1A).

The effect of HBO treatment on ECM genes was further demonstrated through gene set variation analysis (GSVA) using a gene list from GO: 0062023 (collagen containing extracellular matrix); GSVA scores calculated based on this gene list were significantly lower in HBO-treated *vs.* control (normoxia) mice lungs ($P = 0.037$; Fig. 1B). Similar results were obtained using another gene list from GO: 0031012 (extracellular matrix) ($P = 0.039$; Fig. 1C). Together, these results demonstrate the potential impact of HBO treatment on ECM deposition in mice lungs.

Repetitive HBO treatments attenuate bleomycin-induced pulmonary fibrosis in mice.

Given the above observation, we next tested whether HBO exposure could affect the development of pulmonary fibrosis, where aberrant ECM deposition is a key feature. To test this hypothesis, bleomycin-induced pulmonary fibrosis in C57BL/6 mice was used (Supplmentary Fig. 1). HBO exposure was applied daily from day 7, after intratracheal bleomycin instillation until day 20, one day before sample collections (Fig. 2A). Bleomycin-challenged mice showed a clear development of pulmonary fibrosis, with thickened alveoli septae and collagen deposition in the interstitium visualized in H/E stain (Fig. 2B) and Masson’s trichrome stain (Fig. 2C). In contrast, fibrotic areas and collagen deposition were markedly reduced in lungs from bleomycin-challenged mice treated with repetitive HBO (Fig. 2B and C, right panels).

To quantify the severity of fibrosis, Ashcroft scores were evaluated, and a clear reduction was observed in the lungs from bleomycin-challenged mice treated with repetitive HBO compared to those from bleomycin-challenged mice ($P = 0.002$; Fig. 3A). Hydroxyproline is a major component of fibrillar collagen of all types. Consistent with the morphological changes and Ashcroft scores above, hydroxyproline content was significantly reduced in lungs from bleomycin-challenged mice treated with repetitive HBO ($P = 0.009$; Fig. 3B). Effects of HBO on body weight in mice after bleomycin challenge were minimal ($P = 0.820$; Supplementary Fig. 2). Taken together, these data highlight an impact of repetitive HBO exposure on bleomycin-induced pulmonary fibrosis in mice.

Effect of repetitive HBO treatments on fibroblast activation and ECM deposition in mice lungs.

We next checked the expression levels of *Acta2* (encoding α-smooth muscle actin, α-SMA, a myofibroblast marker) and other ECM genes, including *Col1a1* (encoding type I collagen) and *Fn1* (encoding fibronectin) in mice lungs. As expected, the mRNA levels of *Acta2* (α-SMA), *Col1a1* (collagen I) and *Fn1* (fibronectin) were significantly increased in the lungs from bleomycin-challenged mice compared to the control mice (all P values were less than 0.05; Supplementary Fig. 3). When the bleomycin-challenged mice were exposed to repetitive HBO treatments, the mRNA level of *Acta2* (α-SMA) and *Col1a1* were both significantly reduced ($P = 0.005$ and 0.014, respectively; Fig. 4A). Under the same conditions, the expression of *Fn1* was also decreased, although statistical significance was not reached ($P = 0.259$; Fig. 4A). Similar results were obtained when measuring the protein level of α-

SMA using western blot (P = 0.037; Fig. 4B). These results indicate that repetitive HBO exposure could potentially reduce myofibroblast differentiation and activation *in vivo*.

Effect of HBO treatment on TGF-β-induced fibroblast activation and HIF-1α levels in human lung fibroblasts (HFL1).

To validate the findings in *vitro*, the effects of HBO treatment on TGF-β-induced fibroblast activation in human lung fibroblasts HFL1 were examined (Fig. 5A). After incubating HFL1 cells with TGF-β for 48 hours, the mRNA levels of *ACTA2* (α-SMA), *COL1A1* (collagen I) and *FN1*(fibronectin) were all induced in HFL1 cells compared to control cells (all P values were less than 0.05; Supplementary Fig. 3), indicating fibroblasts were activated. TGF-β was then removed and HBO exposure was applied to HFL1 cells for 90 minutes (Fig. 5A). At 72 hours after TGF-β treatment, *ACTA2* (α-SMA), *COL1A1* and *FN1* sustained at high expression levels in TGF-β-treated groups compared to controls (all P values were less than 0.05; Fig. 5B). In TGF-β-treated cells, the mRNA levels of *ACTA2* (α-SMA), *COL1A1* and *FN1* were significantly reduced when exposed to HBO (all P values were less than 0.05; Fig. 5B). In the absence of TGF-β, the mRNA levels of *ACTA2* (α-SMA), *COL1A1* and *FN1* were also decreased when exposed to HBO, although statistical significance was not reached (Fig. 5B). Similar results were obtained when measuring the protein level of α-SMA using western blot (Fig. 5C). In addition, to test if HBO treatment could block TGF-β-induced fibroblast differentiation, HBO exposure was applied immediately following TGF-β treatment (Supplementary Fig. 5A). Q-PCR showed that this treatment could also reduce TGF-β-induced *ACTA2* (α-SMA) mRNA levels in HFL1 cells (P = 0.043) (Supplementary Fig. 5B).These results suggested that HBO exposure could reverse and block, at least partially, TGF-β-induced fibroblast activation.

Finally, we checked the effects of HBO treatment on HIF-1α levels following TGF-β treatment in human lung fibroblasts (Fig. 6A). In consistence with previous studies (Yamazaki et al., 2017; Senavirathna et al., 2020), TGF-β treatment significantly up-regulated the protein levels of HIF-1α in HFL1 (P = 4.9E-4; Fig. 6B and C). As expected, HBO exposure dramatically reduced TGF-β-induced HIF-1α protein expression (P = 3.9E-5; Fig. 6B and C). In addition, we were able to show that HBO exposure can also block TGF-β-induced HIF-1α levels in HFL1 (Supplementary Fig. 5C-E).

Discussion

Pulmonary fibrosis is a chronic, progressive lung disease with limited therapeutic options (Richeldi et al., 2017). In this study we utilised an animal model and assessment methods for pulmonary fibrosis recommended by the American Thoracic Society (Jenkins et al., 2017). We report that repetitive HBO exposure attenuates bleomycin-induced pulmonary fibrosis in mice, and that HBO exposure, both *in vivo* and *in vitro*, inhibits fibroblast activation and ECM production. HBO therapy is generally very safe (Camporesi, 2014; Hadanny et al., 2016; Hadanny et al., 2019) and has been used in a variety of clinical practices (Choudhury, 2018; Kirby, 2019). Together with earlier reports indicating an improvement of pulmonary function in IPF patients following HBO therapy (Ma and Du, 2003; Qiu et al., 2013), our findings support HBO as a potential therapy for patients with pulmonary fibrosis.

As a master regulator of fibroblast activation, it was previously reported that in human lung fibroblasts, TGF-β upregulates the protein levels of HIF-1α, and synergistically increases the expression of myofibroblast markers and ECM genes (Senavirathna et al., 2020). In addition, TGF-β-induced fibroblast activation is suppressed by HIF-1α inhibition in human lung fibroblasts (Yamazaki et al., 2017). With evidence in this study showing the ability of HBO to prevent and reverse TGF-β-induced HIF-1α expression, we propose that HBO exposure affects TGF-β-induced fibroblast activation by modulating the expression of HIF-1α.

In addition to the effect of counteracting the upregulation of HIF-1α induced by TGF-β, HBO is reported to reduce HIF-1α levels through alleviating tissue hypoxia, in a similar manner to multiple ischemic conditions, injuries and inflammatory conditions (Li et al., 2005; Calvert et al., 2006; Sun et al., 2008; Bai et al., 2009; Zhou et al., 2013). Hypoxia is a hallmark of pulmonary fibrosis. Previously, studies have shown that the hypoxia signaling pathway was activated in IPF patients (Tzouvelekis et al., 2007; Ueno et al., 2011; Xie et al., 2013; Qian et al., 2015; Kusko et al., 2016; Philip et al., 2017; Yamazaki et al., 2017; Burman et al., 2018; Aquino-Galvez et al., 2019), Further, chronic exposure to hypoxic conditions can increase the severity of bleomycin-induced pulmonary fibrosis in murine models (Braun et al., 2018; Burman et al., 2018; Gille et al., 2018). Furthermore, inhibition of HIF-1α, directly or indirectly, alleviates pulmonary fibrosis in the bleomycin-induced model (Yamazaki et al., 2017; Goodwin et al., 2018; Strowitzki et al., 2019; Kseibati et al., 2020). Also, hypoxia induced fibroblast differentiation directly and this effect depended on HIF-1α (Robinson et al., 2012; Lv et al., 2018). HBO is an effective way of oxygenating hypoxic tissues through increasing the dissolved oxygen in plasma and amplifying oxygen diffusion distance under higher pressure. Its effect on alleviating tissue hypoxia has been confirmed in solid tumors (Kinoshita et al., 2000; Beppu et al., 2002; Thews and Vaupel, 2016) and focal cerebral ischemia tissue (Sun et al., 2008).

Given both hypoxia and TGF-β signaling pathway are activated in pulmonary fibrosis, HBO may inhibit HIF-1α expression induced by both hypoxia and TGF-β. Previous studies suggested that the effect on alleviating tissue hypoxia by HBO can only maintain for a certain time (Kinoshita et al., 2000; Beppu et al., 2002; Thews and Vaupel, 2016), suggesting that repetitive HBO exposure is required. Future studies are needed to optimise the protocol for the clinical application of applying HBO as a therapy for pulmonary fibrosis.

In summary, this study provides evidence that HBO exposure attenuates bleomycin-induced pulmonary fibrosis *in vivo* and TGF-β-induced fibroblast activation *in vitro*. Mechanistically, this effect may be mediated by down-regulating TGF-β-induced expression of HIF-1α. These findings support HBO as a potential life-changing therapy for patients with pulmonary fibrosis, although further research is needed to fully evaluate this.

Conflict of Interest

The authors declare that the research was conducted in the absence of any commercial or financial relationships that could be construed as a potential conflict of interest.

Author Contributions

YW, ZJ, YY and YL conceived and designed the experiments. YY, YL, GQ, YZ and ZX conducted the experiments. YY, YZ analyzed the data. YY, YW, YL and CH wrote the manuscript. All authors read and approved the manuscript.

Funding

YY was supported by Natural Science Fund for Colleges and Universities in Jiangsu Province (19KJB320002), the Science and Technology Planning Project of Nantong Municipality, China (JC2020010) and a Research Startup Fund of Nantong University. YZ was supported by an Institute for Life Sciences PhD Studentship. ZX was supported by China Scholarship Council. CH was supported by Gerald Kerkut Charitable Trust and University of Southampton Central VC Scholarship Scheme. ZJ was supported by the National Natural Science Foundation of China (81671859 and 81601639) and Natural Science Foundation of Jiangsu Province (BK20161282). YW was supported by Medical Research Council (MR/S025480/1).

References

Aquino-Galvez, A., Gonzalez-Avila, G., Jimenez-Sanchez, L.L., Maldonado-Martinez, H.A., Cisneros, J., Toscano-Marquez, F., et al. (2019). Dysregulated expression of hypoxia-inducible factors augments myofibroblasts differentiation in idiopathic pulmonary fibrosis. *Respir Res* 20(1)**,** 130. doi: 10.1186/s12931-019-1100-4.

Bai, X., Sun, B., Pan, S., Jiang, H., Wang, F., Krissansen, G.W., et al. (2009). Down-regulation of hypoxia-inducible factor-1alpha by hyperbaric oxygen attenuates the severity of acute pancreatitis in rats. *Pancreas* 38(5)**,** 515-522. doi: 10.1097/MPA.0b013e31819cac24.

Bell, E.C., Cox, N.S., Goh, N., Glaspole, I., Westall, G.P., Watson, A., et al. (2017). Oxygen therapy for interstitial lung disease: a systematic review. *Eur Respir Rev* 26(143)**,** 160080. doi: 10.1183/16000617.0080-2016.

Beppu, T., Kamada, K., Yoshida, Y., Arai, H., Ogasawara, K., and Ogawa, A. (2002). Change of oxygen pressure in glioblastoma tissue under various conditions. *J Neurooncol* 58(1)**,** 47-52. doi: 10.1023/a:1015832726054.

Braun, R.K., Broytman, O., Braun, F.M., Brinkman, J.A., Clithero, A., Modi, D., et al. (2018). Chronic intermittent hypoxia worsens bleomycin-induced lung fibrosis in rats. *Respir Physiol Neurobiol* 256**,** 97-108. doi: 10.1016/j.resp.2017.04.010.

Burman, A., Kropski, J.A., Calvi, C.L., Serezani, A.P., Pascoalino, B.D., Han, W., et al. (2018). Localized hypoxia links ER stress to lung fibrosis through induction of C/EBP homologous protein. *JCI Insight* 3(16)**,** e99543. doi: 10.1172/jci.insight.99543.

Calvert, J.W., Cahill, J., Yamaguchi-Okada, M., and Zhang, J.H. (2006). Oxygen treatment after experimental hypoxia-ischemia in neonatal rats alters the expression of HIF-1alpha and its downstream target genes. *J Appl Physiol (1985)* 101(3)**,** 853-865. doi: 10.1152/japplphysiol.00268.2006.

Camporesi, E.M. (2014). Side effects of hyperbaric oxygen therapy. *Undersea Hyperb Med* 41(3)**,** 253-257.

Choudhury, R. (2018). Hypoxia and hyperbaric oxygen therapy: a review. *Int J Gen Med* 11**,** 431-442. doi: 10.2147/IJGM.S172460.

Dowman, L.M., McDonald, C.F., Bozinovski, S., Vlahos, R., Gillies, R., Pouniotis, D., et al. (2017). Greater endurance capacity and improved dyspnoea with acute oxygen supplementation in idiopathic pulmonary fibrosis patients without resting hypoxaemia. *Respirology* 22(5)**,** 957-964. doi: 10.1111/resp.13002.

Faverio, P., De Giacomi, F., Bonaiti, G., Stainer, A., Sardella, L., Pellegrino, G., et al. (2019). Management of Chronic Respiratory Failure in Interstitial Lung Diseases: Overview and Clinical Insights. *Int J Med Sci* 16(7)**,** 967-980. doi: 10.7150/ijms.32752.

George, P.M., Wells, A.U., and Jenkins, R.G. (2020). Pulmonary fibrosis and COVID-19: the potential role for antifibrotic therapy. *The Lancet Respiratory Medicine* 8(8)**,** 807-815. doi: 10.1016/S2213-2600(20)30225-3.

Gille, T., Didier, M., Rotenberg, C., Delbrel, E., Marchant, D., Sutton, A., et al. (2018). Intermittent Hypoxia Increases the Severity of Bleomycin-Induced Lung Injury in Mice. *Oxid Med Cell Longev* 2018**,** 1240192. doi: 10.1155/2018/1240192.

Goodwin, A.T., and Jenkins, G. (2016). Molecular Endotyping of Pulmonary Fibrosis. *Chest* 149(1)**,** 228-237. doi: 10.1378/chest.15-1511.

Goodwin, J., Choi, H., Hsieh, M.H., Neugent, M.L., Ahn, J.M., Hayenga, H.N., et al. (2018). Targeting Hypoxia-Inducible Factor-1alpha/Pyruvate Dehydrogenase Kinase 1 Axis by Dichloroacetate Suppresses Bleomycin-induced Pulmonary Fibrosis. *Am J Respir Cell Mol Biol* 58(2)**,** 216-231. doi: 10.1165/rcmb.2016-0186OC.

Hadanny, A., Meir, O., Bechor, Y., Fishlev, G., Bergan, J., and Efrati, S. (2016). The safety of hyperbaric oxygen treatment--retrospective analysis in 2,334 patients. *Undersea Hyperb Med* 43(2)**,** 113-122.

Hadanny, A., Zubari, T., Tamir-Adler, L., Bechor, Y., Fishlev, G., Lang, E., et al. (2019). Hyperbaric oxygen therapy effects on pulmonary functions: a prospective cohort study. *BMC Pulm Med* 19(1)**,** 148. doi: 10.1186/s12890-019-0893-8.

Hanzelmann, S., Castelo, R., and Guinney, J. (2013). GSVA: gene set variation analysis for microarray and RNA-seq data. *BMC Bioinformatics* 14**,** 7. doi: 10.1186/1471-2105-14-7.

Hubner, R.H., Gitter, W., El Mokhtari, N.E., Mathiak, M., Both, M., Bolte, H., et al. (2008). Standardized quantification of pulmonary fibrosis in histological samples. *Biotechniques* 44(4)**,** 507-511, 514-507. doi: 10.2144/000112729.

Jenkins, R.G., Moore, B.B., Chambers, R.C., Eickelberg, O., Konigshoff, M., Kolb, M., et al. (2017). An Official American Thoracic Society Workshop Report: Use of Animal Models for the Preclinical Assessment of Potential Therapies for Pulmonary Fibrosis. *Am J Respir Cell Mol Biol* 56(5)**,** 667-679. doi: 10.1165/rcmb.2017-0096ST.

Kinoshita, Y., Kohshi, K., Kunugita, N., Tosaki, T., and Yokota, A. (2000). Preservation of tumour oxygen after hyperbaric oxygenation monitored by magnetic resonance imaging. *Br J Cancer* 82(1)**,** 88-92. doi: 10.1054/bjoc.1999.0882.

Kirby, J.P. (2019). Hyperbaric Oxygen Therapy as an Elective Treatment. *Mo Med* 116(3)**,** 184-187.

Koyauchi, T., Hasegawa, H., Kanata, K., Kakutani, T., Amano, Y., Ozawa, Y., et al. (2018). Efficacy and Tolerability of High-Flow Nasal Cannula Oxygen Therapy for Hypoxemic Respiratory Failure in Patients with Interstitial Lung Disease with Do-Not-Intubate Orders: A Retrospective Single-Center Study. *Respiration* 96(4)**,** 323-329. doi: 10.1159/000489890.

Kseibati, M.O., Shehatou, G.S.G., Sharawy, M.H., Eladl, A.E., and Salem, H.A. (2020). Nicorandil ameliorates bleomycin-induced pulmonary fibrosis in rats through modulating eNOS, iNOS, TXNIP and HIF-1alpha levels. *Life Sci* 246**,** 117423. doi: 10.1016/j.lfs.2020.117423.

Kusko, R.L., Brothers, J.F., 2nd, Tedrow, J., Pandit, K., Huleihel, L., Perdomo, C., et al. (2016). Integrated Genomics Reveals Convergent Transcriptomic Networks Underlying Chronic Obstructive Pulmonary Disease and Idiopathic Pulmonary Fibrosis. *Am J Respir Crit Care Med* 194(8)**,** 948-960. doi: 10.1164/rccm.201510-2026OC.

Lam, G., Fontaine, R., Ross, F.L., and Chiu, E.S. (2017). Hyperbaric Oxygen Therapy: Exploring the Clinical Evidence. *Adv Skin Wound Care* 30(4)**,** 181-190. doi: 10.1097/01.ASW.0000513089.75457.22.

Li, Y., Zhou, C., Calvert, J.W., Colohan, A.R., and Zhang, J.H. (2005). Multiple effects of hyperbaric oxygen on the expression of HIF-1 alpha and apoptotic genes in a global ischemia-hypotension rat model. *Exp Neurol* 191(1)**,** 198-210. doi: 10.1016/j.expneurol.2004.08.036.

Lv, X.M., Li, M.D., Cheng, S., Liu, B.L., Liu, K., Zhang, C.F., et al. (2018). Neotuberostemonine inhibits the differentiation of lung fibroblasts into myofibroblasts in mice by regulating HIF-1alpha signaling. *Acta Pharmacol Sin* 39(9)**,** 1501-1512. doi: 10.1038/aps.2017.202.

Ma, Y., and Du, J. (2003). Hyperbaric oxygen treatment on idiopathic pulmonary fibrosis: clinical observation of 67 cases. *Shandong Medical Journal* 43(1)**,** 34.

Meltzer, E.B., and Noble, P.W. (2008). Idiopathic pulmonary fibrosis. *Orphanet J Rare Dis* 3**,** 8. doi: 10.1186/1750-1172-3-8.

Oscarsson, N., Ny, L., Molne, J., Lind, F., Ricksten, S.E., Seeman-Lodding, H., et al. (2017). Hyperbaric oxygen treatment reverses radiation induced pro-fibrotic and oxidative stress responses in a rat model. *Free Radic Biol Med* 103**,** 248-255. doi: 10.1016/j.freeradbiomed.2016.12.036.

Philip, K., Mills, T.W., Davies, J., Chen, N.Y., Karmouty-Quintana, H., Luo, F., et al. (2017). HIF1A up-regulates the ADORA2B receptor on alternatively activated macrophages and contributes to pulmonary fibrosis. *FASEB J* 31(11)**,** 4745-4758. doi: 10.1096/fj.201700219R.

Qian, F., He, M., Duan, W., Mao, L., Li, Q., Yu, Z., et al. (2015). Cross regulation between hypoxia-inducible transcription factor-1α (HIF-1α) and transforming growth factor (TGF)-β1 mediates nickel oxide nanoparticles (NiONPs)-induced pulmonary fibrosis. *Am J Transl Res* 7(11)**,** 2364-2378.

Qiu, X., Huang, H., and Jin, N. (2013). Obervation of effect of hyperbaric oxygen therapy on serum fibrosis associated indexes and pulmonary function in idiopathic pulmonary fibrosis patients. *Journal of Hainan Medical University* 19(8)**,** 1054.

Richeldi, L., Collard, H.R., and Jones, M.G. (2017). Idiopathic pulmonary fibrosis. *Lancet* 389(10082)**,** 1941-1952. doi: 10.1016/S0140-6736(17)30866-8.

Robinson, C.M., Neary, R., Levendale, A., Watson, C.J., and Baugh, J.A. (2012). Hypoxia-induced DNA hypermethylation in human pulmonary fibroblasts is associated with Thy-1 promoter methylation and the development of a pro-fibrotic phenotype. *Respir Res* 13**,** 74. doi: 10.1186/1465-9921-13-74.

Senavirathna, L.K., Huang, C., Pushparaj, S., Xu, D., and Liu, L. (2020). Hypoxia and transforming growth factor beta1 regulation of long non-coding RNA transcriptomes in human pulmonary fibroblasts. *Physiol Rep* 8(1)**,** e14343. doi: 10.14814/phy2.14343.

Strowitzki, M.J., Ritter, A.S., Kimmer, G., and Schneider, M. (2019). Hypoxia-adaptive pathways: A pharmacological target in fibrotic disease? *Pharmacol Res* 147**,** 104364. doi: 10.1016/j.phrs.2019.104364.

Sun, L., Marti, H.H., and Veltkamp, R. (2008). Hyperbaric oxygen reduces tissue hypoxia and hypoxia-inducible factor-1 alpha expression in focal cerebral ischemia. *Stroke* 39(3)**,** 1000-1006. doi: 10.1161/STROKEAHA.107.490599.

Thews, O., and Vaupel, P. (2016). Temporal changes in tumor oxygenation and perfusion upon normo- and hyperbaric inspiratory hyperoxia. *Strahlenther Onkol* 192(3)**,** 174-181. doi: 10.1007/s00066-015-0916-1.

Tzouvelekis, A., Harokopos, V., Paparountas, T., Oikonomou, N., Chatziioannou, A., Vilaras, G., et al. (2007). Comparative expression profiling in pulmonary fibrosis suggests a role of hypoxia-inducible factor-1alpha in disease pathogenesis. *Am J Respir Crit Care Med* 176(11)**,** 1108-1119. doi: 10.1164/rccm.200705-683OC.

Ueno, M., Maeno, T., Nomura, M., Aoyagi-Ikeda, K., Matsui, H., Hara, K., et al. (2011). Hypoxia-inducible factor-1alpha mediates TGF-beta-induced PAI-1 production in alveolar macrophages in pulmonary fibrosis. *Am J Physiol Lung Cell Mol Physiol* 300(5)**,** L740-752. doi: 10.1152/ajplung.00146.2010.

Vandivort, T.C., An, D., and Parks, W.C. (2016). An Improved Method for Rapid Intubation of the Trachea in Mice. *J Vis Exp* (108)**,** 53771. doi: 10.3791/53771.

Visca, D., Mori, L., Tsipouri, V., Fleming, S., Firouzi, A., Bonini, M., et al. (2018). Effect of ambulatory oxygen on quality of life for patients with fibrotic lung disease (AmbOx): a prospective, open-label, mixed-method, crossover randomised controlled trial. *Lancet Respir Med* 6(10)**,** 759-770. doi: 10.1016/S2213-2600(18)30289-3.

Xie, H., Tan, J.T., Wang, R.L., Meng, X.X., Tang, X., and Gao, S. (2013). Expression and significance of HIF-1alpha in pulmonary fibrosis induced by paraquat. *Exp Biol Med (Maywood)* 238(9)**,** 1062-1068. doi: 10.1177/1535370213498978.

Yamazaki, R., Kasuya, Y., Fujita, T., Umezawa, H., Yanagihara, M., Nakamura, H., et al. (2017). Antifibrotic effects of cyclosporine A on TGF-beta1-treated lung fibroblasts and lungs from bleomycin-treated mice: role of hypoxia-inducible factor-1alpha. *FASEB J* 31(8)**,** 3359-3371. doi: 10.1096/fj.201601357R.

Yuan, Y., Zhou, Y., Li, Y., Hill, C., Ewing, R.M., Jones, M.G., et al. (2020). Deconvolution of RNA-Seq Analysis of Hyperbaric Oxygen-Treated Mice Lungs Reveals Mesenchymal Cell Subtype Changes. *Int J Mol Sci* 21(4)**,** 1371. doi: 10.3390/ijms21041371.

Zhou, Y., Liu, X.H., Qu, S.D., Yang, J., Wang, Z.W., Gao, C.J., et al. (2013). Hyperbaric oxygen intervention on expression of hypoxia-inducible factor-1alpha and vascular endothelial growth factor in spinal cord injury models in rats. *Chin Med J (Engl)* 126(20)**,** 3897-3903. doi: 10.3760/cma.j.issn.0366-6999.20130571.

Zou, R.H., Kass, D.J., Gibson, K.F., and Lindell, K.O. (2020). The Role of Palliative Care in Reducing Symptoms and Improving Quality of Life for Patients with Idiopathic Pulmonary Fibrosis: A Review. *Pulm Ther* 6(1)**,** 35-46. doi: 10.1007/s41030-019-00108-2.

Figure Legends

Figure 1. Repetitive HBO treatments down-regulate extracellular matrix gene expression in mouse lungs.

(A) REVIGO TreeMap showing Gene Ontology (GO) analysis of down-regulated differentially expressed genes (DEGs) in mice lungs exposed to repetitive HBO (GSE143348). Common colours represent groupings based on parent GO terms, and each rectangle is proportional to the relative enrichment of the GO term compared to the whole genome. Genes with false discovery rate (FDR) < 0.05 were considered as DEGs. **(B)** and **(C)** Graphs showing GSVA scores calculated based on gene lists from GO: 0062023 (collagen containing extracellular matrix) **(B)** or GO:0031012 (extracellular matrix) **(C)** in HBO-treated and control lungs. Data were analyzed with unpaired t-test. Data are mean ± s.d., with *P* values indicated. n = 4 samples per group.

Figure 2. Repetitive HBO treatments reduce the fibrotic area and collagen content in bleomycin-challenged mice lungs.

(A) Schematic diagram of the experimental procedure (details in *Methods*). **(B)** and **(C)** Lung tissues from bleomycin-challenged mice (Bleo) or bleomycin-challenged mice treated with repetitive HBO exposure (Bleo + HBO) were stained with H/E **(B)** or Masson's trichrome stain **(C**, collagen shown in blue**)**. In **(B)** and **(C)**, top panels show the whole left lung lobes (scale bar: 1 mm) with higher-magnification images in bottom panels (scale bar: 100 μm).

Figure 3. Repetitive HBO treatments attenuate bleomycin-induced pulmonary fibrosis in mice.

(A) Ashcroft scores in lungs from bleomycin-challenged mice (Bleo) or bleomycin-challenged mice treated with repetitive HBO (Bleo + HBO). Numbers of mice within each group and *P* value are indicated. **(B)** Graph showing relative hydroxyproline content in lungs from bleomycin-challenged mice (Bleo) or bleomycin-challenged mice treated with repetitive HBO (Bleo + HBO). Lung tissue mass-normalised hydroxyproline levels in Bleo group were used to set the baseline value at unity. Data are mean ± s.d., with numbers of mice within each group and *P* value indicated. Data in **(A)** were analysed with unpaired *t*-test. Data in **(B)** were analysed with nonparametric t-test (Mann-Whitney test).

Figure 4. Effects of repetitive HBO treatments on fibroblast activation and ECM deposition in mice lungs.

(A) Fold change in the mRNA levels of *Acta2* (α-SMA), *Col1a1* (collagen I) and *Fn1* (fibronectin) in the lungs from bleomycin-challenged mice (Bleo) or bleomycin-challenged mice treated with repetitive HBO (Bleo + HBO). *Actb* (β-actin) -normalized mRNA levels in the Bleo group were used to set the baseline value at unity. Data are mean ± s.d., with numbers of mice within each group and *P* value indicated. **(B)** Protein expression of α-SMA in lungs from bleomycin-challenged mice (Bleo) or bleomycin-challenged mice treated with repetitive HBO (Bleo + HBO). β-actin was used as a loading control. In the graph, β-actin-normalised protein levels in Bleo group were used to set the baseline value at unity. Data are mean ± s.d., with numbers of mice within each group and *P* value indicated. Data in **(A)** were analysed with unpaired multiple *t*-test. Data in **(B)** were analysed with unpaired *t*-test.

Figure 5. Effects of HBO treatment on TGF-β-induced fibroblast activation in HFL1 cells.

(A) Schematic diagram of the experimental procedure. In brief, TGF-β (5 ng/mL) was added to HFL1 cells for 48 hours to induce fibroblast activation, after which TGF-β was removed, and cells were exposed to 2.5 ATA HBO for 90 minutes immediately. Samples were collected at 72 hours after the

beginning of TGF-β treatment. **(B)** Fold change in the mRNA levels of *ACTA2* (α-SMA), *COL1A1* (collagen I) and *FN1*(fibronectin) in HFL1 cells with indicated treatments. *ACTB* (β-actin)-normalized mRNA levels in control cells (Vehicle) were used to set the baseline value at unity. **(C)** Protein expression of α-SMA in HFL1 cells with indicated treatments. β-actin was used as a loading control. In the graph, β-actin-normalised protein levels in control cells (Vehicle) were used to set the baseline value at unity. Data in **(B)** and **(C)** are mean ± s.d., with *P* values indicated. n = 3 samples each group. Data were analysed with one-way ANOVA.

Figure 6. Effects of HBO treatment on TGF-β-induced HIF-1α expression in HFL1 cells.

(A) Schematic diagram of the experimental procedure. In brief, TGF-β (5 ng/mL) was added to HFL1 cells for 48 hours to induce fibroblast activation, after which TGF-β was removed, followed 2.5 ATA HBO exposure for 90 minutes immediately. Samples were collected at the end of HBO exposure. **(B)** Protein expression of HIF-1α in HFL1 cells with indicated treatments. β-actin was used as a loading control. **(C)** Fold change in the protein level of HIF-1α in HFL1 cells with indicated treatments. β-actin-normalised protein levels in control cells (Vehicle) were used to set the baseline value at unity. Data are mean ± s.d., with *P* values indicated. n = 3 samples each group. Data were analyzed with one-way ANOVA.

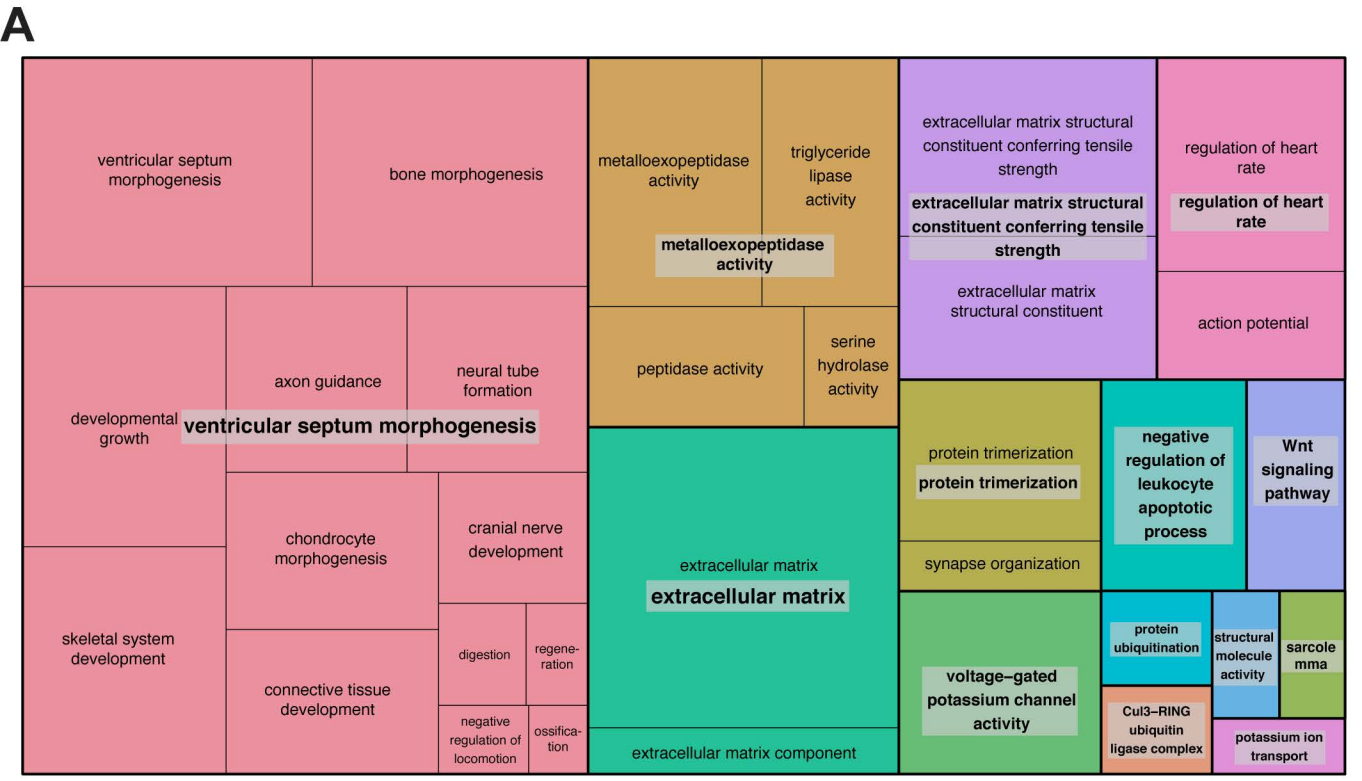
A
ventricular septum morphogenesis
bone morphogenesis
metalloexopeptidase activity
triglyceride lipase activity
metalloexopeptidase activity
extracellular matrix structural constituent conferring tensile strength
extracellular matrix structural constituent conferring tensile strength
regulation of heart rate
regulation of heart rate
extracellular matrix structural constituent
action potential
peptidase activity
serine hydrolase activity
axon guidance
neural tube formation
developmental growth
ventricular septum morphogenesis
protein trimerization
protein trimerization
negative regulation of leukocyte apoptotic process
Wnt signaling pathway
chondrocyte morphogenesis
cranial nerve development
extracellular matrix
extracellular matrix
synapse organization
skeletal system development
digestion
regene-ration
connective tissue development
voltage–gated potassium channel activity
protein ubiquitination
structural molecule activity
sarcole mma
Cul3–RING ubiquitin ligase complex
potassium ion transport
negative regulation of locomotion
ossifica-tion
extracellular matrix component

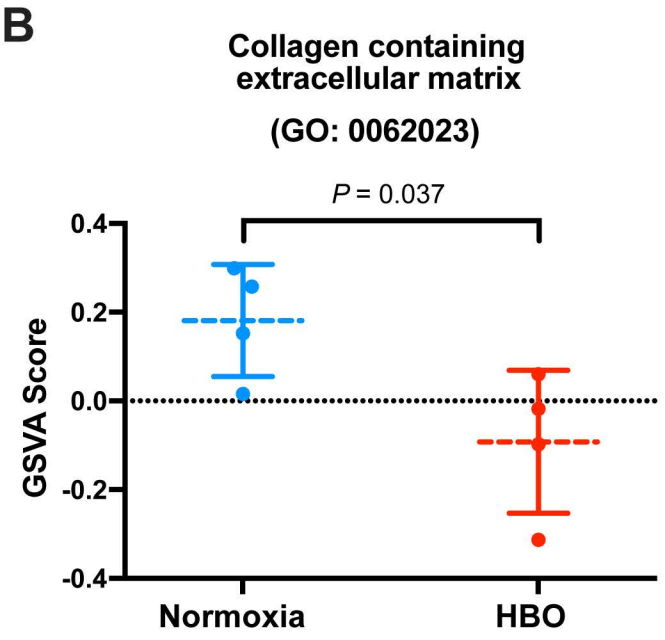
B
Collagen containing extracellular matrix
(GO: 0062023)
P = 0.037
GSVA Score
0.4
0.2
0.0
-0.2
-0.4
Normoxia
HBO

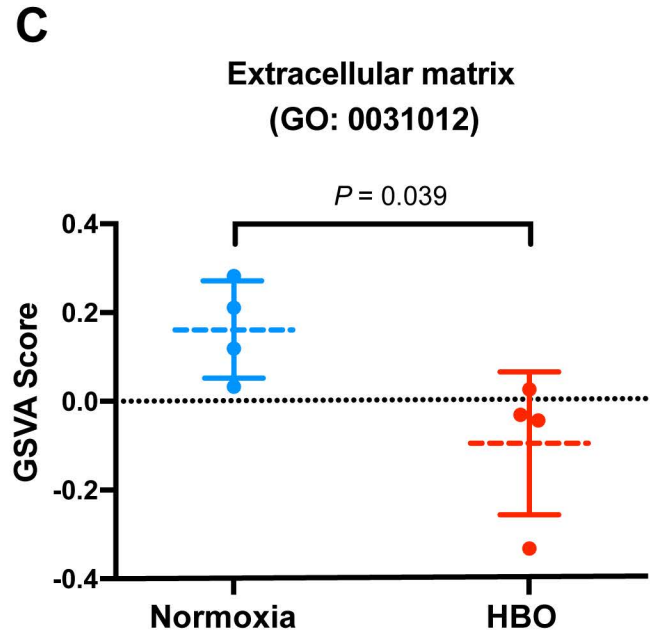
C
Extracellular matrix
(GO: 0031012)
P = 0.039
GSVA Score
0.4
0.2
0.0
-0.2
-0.4
Normoxia
HBO

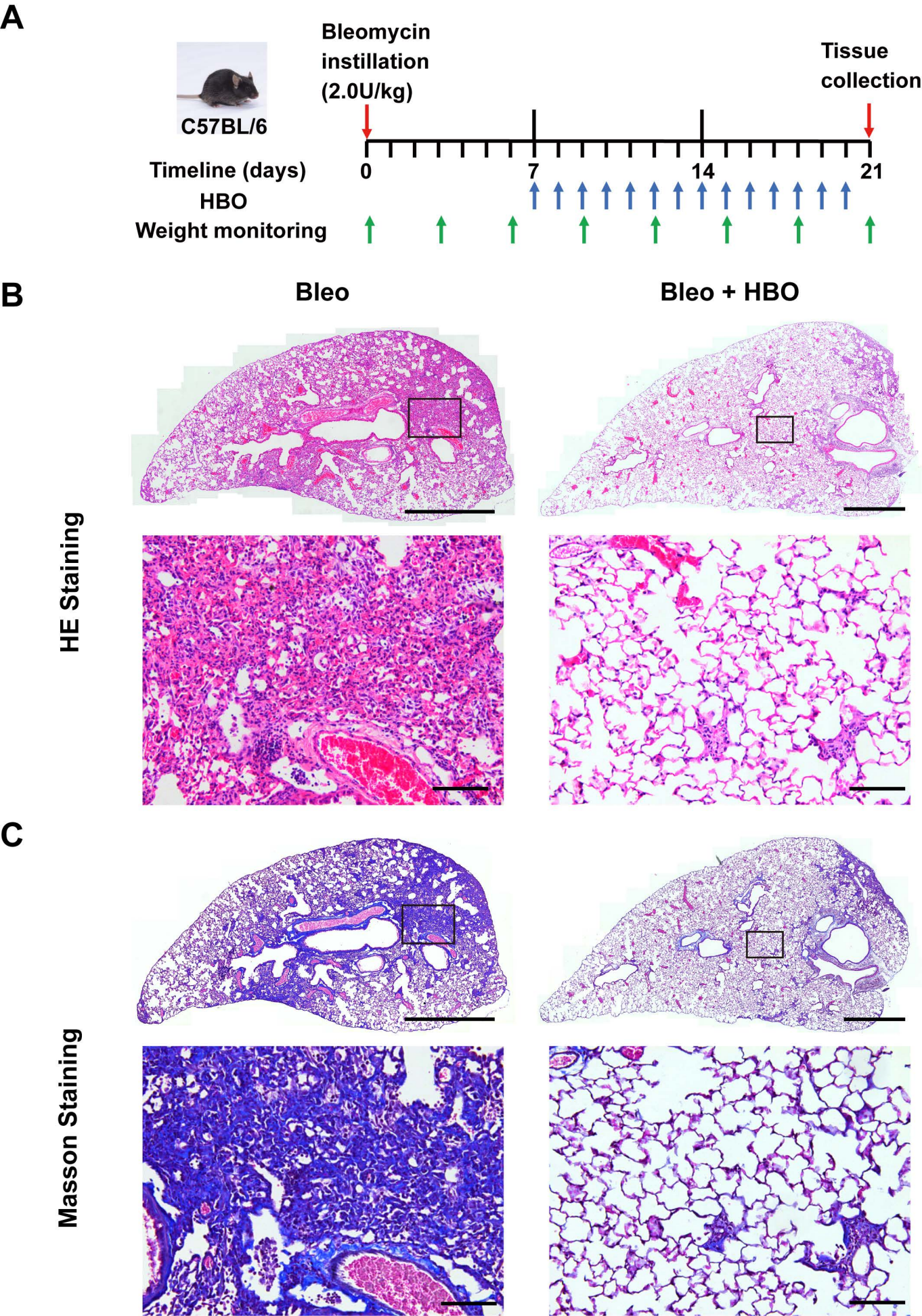
A
C57BL/6
Bleomycin instillation (2.0U/kg)
Tissue collection
Timeline (days)
HBO
Weight monitoring
0
7
14
21
B
Bleo
Bleo + HBO
HE Staining
C
Masson Staining

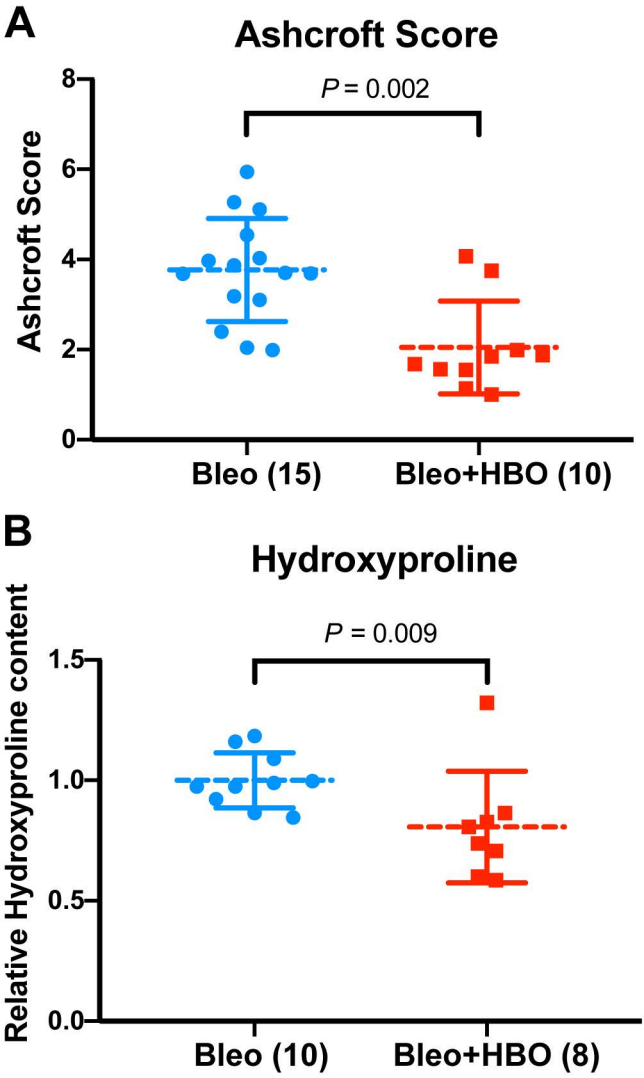
A
Ashcroft Score
P = 0.002
Ashcroft Score
8
6
4
2
0
Bleo (15)
Bleo+HBO (10)
B
Hydroxyproline
P = 0.009
Relative Hydroxyproline content
1.5
1.0
0.5
0.0
Bleo (10)
Bleo+HBO (8)

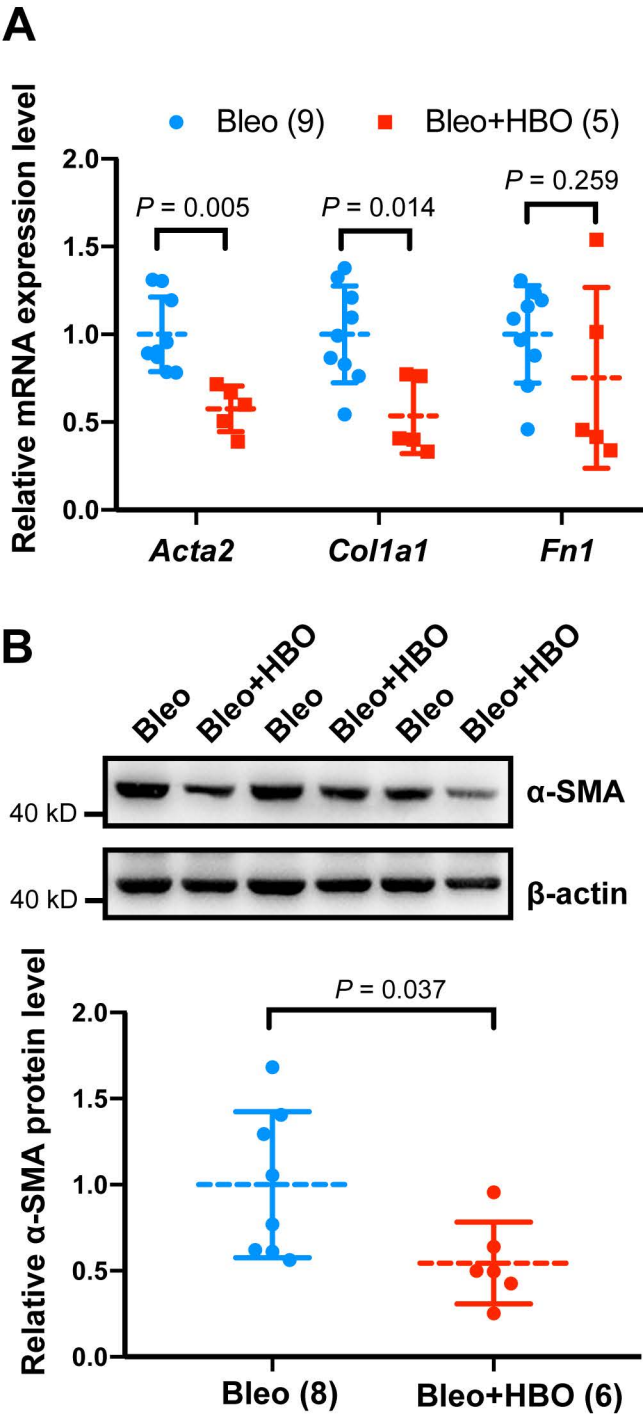
A
Bleo (9)
Bleo+HBO (5)
Relative mRNA expression level
2.0
1.5
1.0
0.5
0.0
P = 0.005
P = 0.014
P = 0.259
Acta2
Col1a1
Fn1
B
Bleo
Bleo+HBO
Bleo
Bleo+HBO
Bleo
Bleo+HBO
40 kD
α-SMA
40 kD
β-actin
Relative α-SMA protein level
2.0
1.5
1.0
0.5
0.0
P = 0.037
Bleo (8)
Bleo+HBO (6)

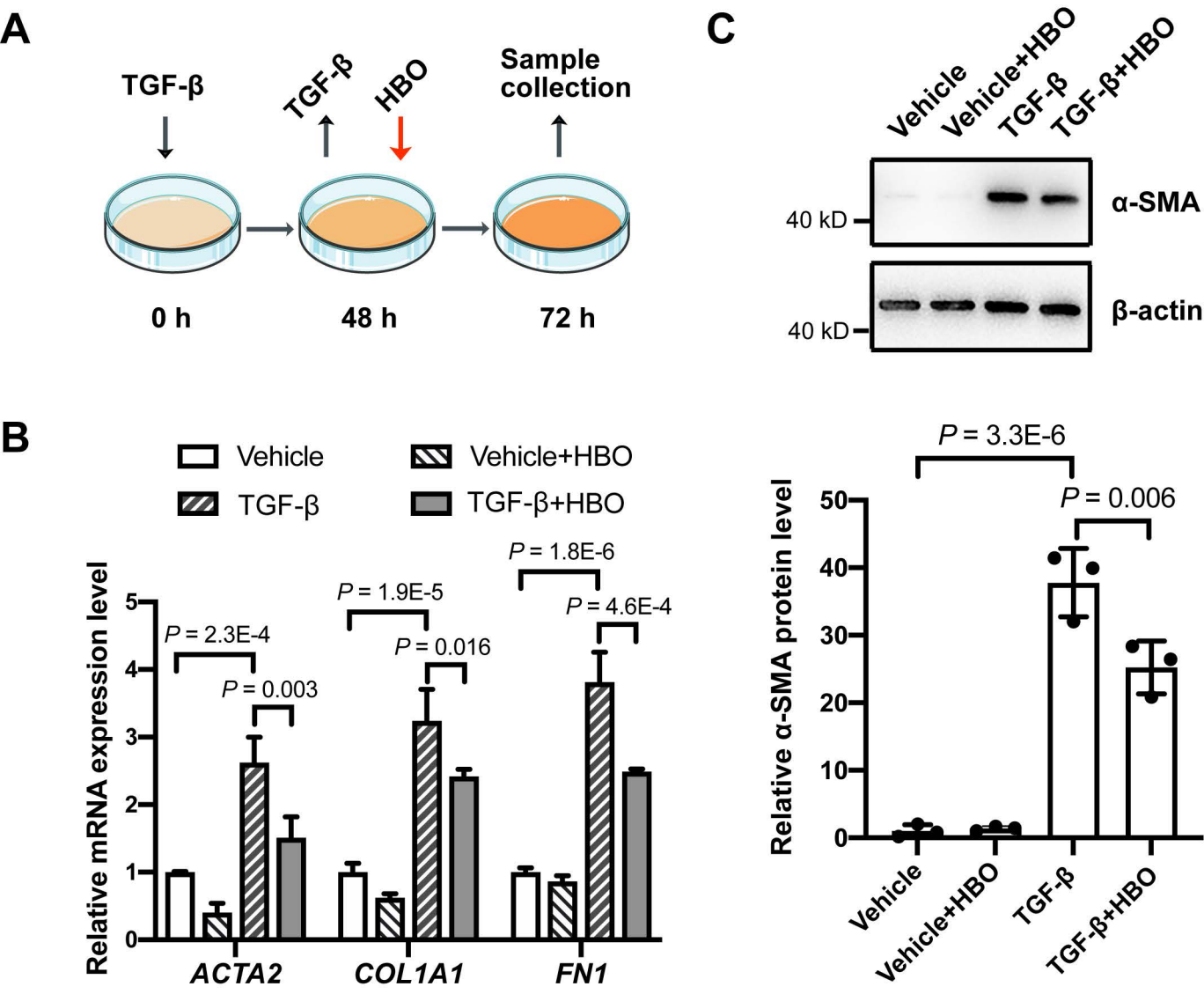
A
TGF-β
TGF-β
HBO
Sample collection
0 h
48 h
72 h
B
Vehicle
Vehicle+HBO
TGF-β
TGF-β+HBO
Relative mRNA expression level
P = 2.3E-4
P = 0.003
P = 1.9E-5
P = 0.016
P = 1.8E-6
P = 4.6E-4
ACTA2
COL1A1
FN1
C
Vehicle
Vehicle+HBO
TGF-β
TGF-β+HBO
40 kD
α-SMA
40 kD
β-actin
Relative α-SMA protein level
P = 3.3E-6
P = 0.006

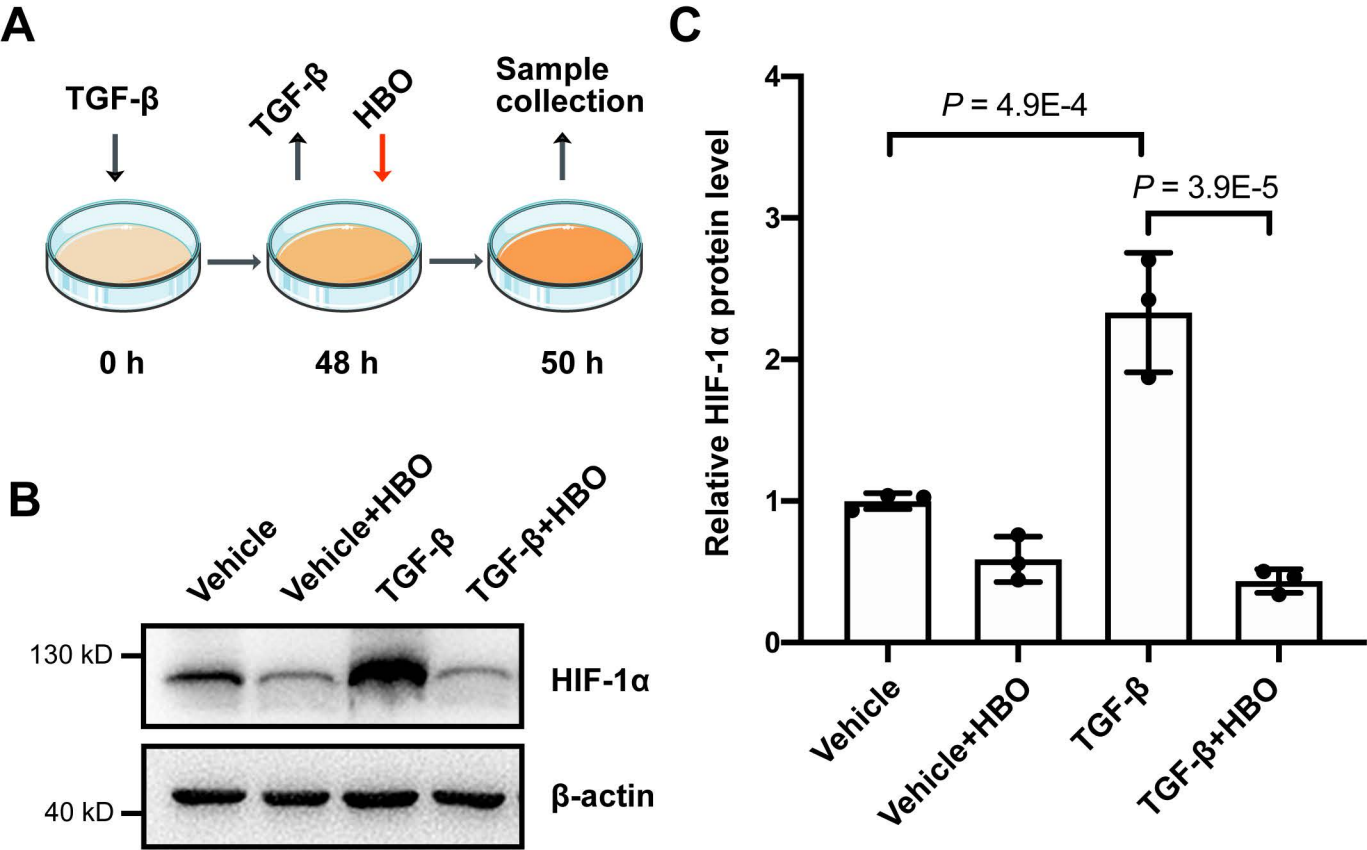
A
TGF-β
TGF-β
HBO
Sample collection
0 h
48 h
50 h
B
Vehicle
Vehicle+HBO
TGF-β
TGF-β+HBO
130 kD
HIF-1α
40 kD
β-actin
C
Relative HIF-1α protein level
P = 4.9E-4
P = 3.9E-5
0
1
2
3
4
Vehicle
Vehicle+HBO
TGF-β
TGF-β+HBO

Supplementary Material

Supplementary Figures

Supplementary Figure 1. Bleomycin treatment induces pulmonary fibrosis in mice.

Supplementary Figure 2. Body weight changes in bleomycin-challenged mice (Bleo) or bleomycin-challenged mice treated with repetitive HBO (Bleo + HBO).

Supplementary Figure 3. Effects of bleomycin on fibroblast activation and ECM deposition in mice lungs.

Supplementary Figure 4. Effects of TGF-β on fibroblast activation in HFL1 cells.

Supplementary Figure 5. Effects of HBO treatment on TGF-β-induced fibroblast differentiation and HIF-1α expression.

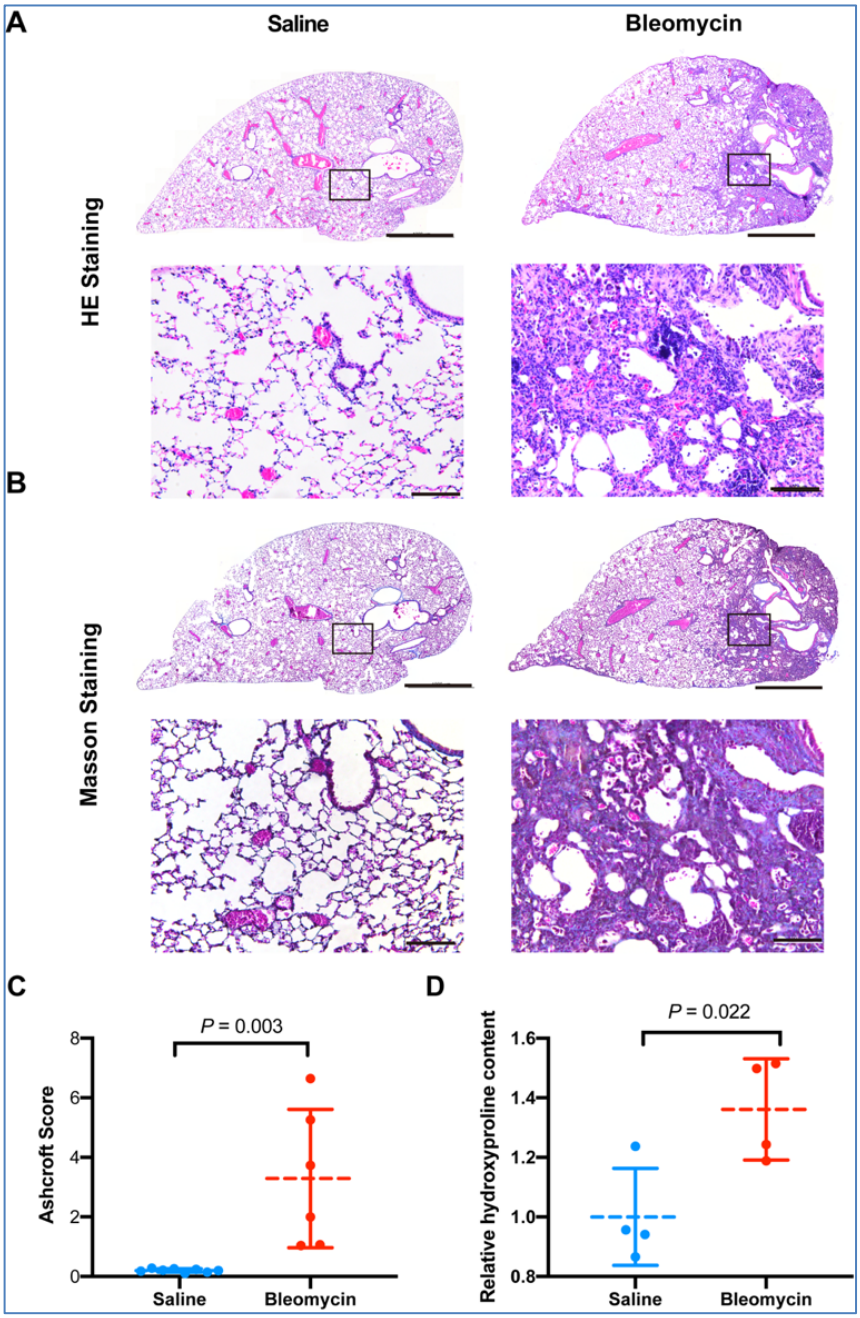

Supplementary Figure 1. Bleomycin treatment induces pulmonary fibrosis in mice. (A and **B)** Lungs from saline-treated (Saline) or bleomycin-challenged mice (Bleomycin) collected at day 21 post instillation were stained with H/E **(A)** or Masson's trichrome stain **(B**, collagen shown in blue**)**. Top panels show the whole left lung lobe (scale bar: 1 mm) with higher-magnification images in bottom panels (scale bar: 100 μm). **(C)** Graph showing Ashcroft scores in lungs from saline-treated (Saline) or bleomycin-challenged (Bleomycin) mice. **(D)** Graph showing relative hydroxyproline content in lungs from saline-treated (Saline) or bleomycin-challenged (Bleomycin) mice. Lung tissue mass-normalised hydroxyproline levels in saline group were used to set the baseline value at unity. Data are mean ± s.d., with *P* values analysed with unpaired *t*-test.

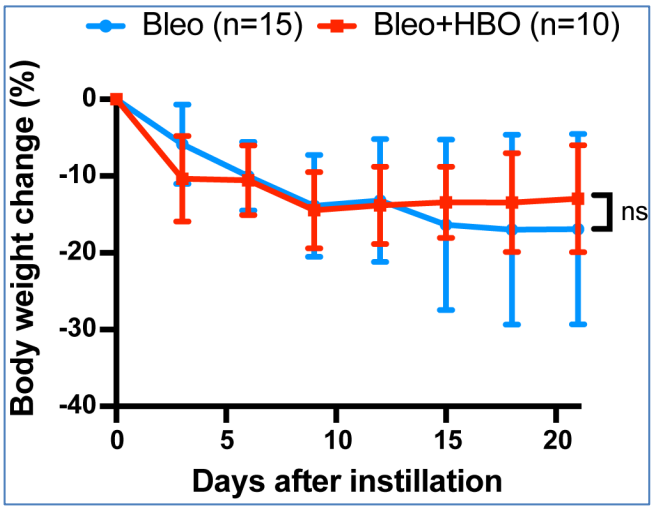

Supplementary Figure 2. Body weight changes in bleomycin-challenged mice (Bleo) or bleomycin-challenged mice treated with repetitive HBO (Bleo + HBO). Body weights were measured every third day. A Two-way ANOVA test with repeated measure data was used to analyse the difference with no significant (ns) difference identified. Data are mean ± s.d., with numbers of mice within each group indicated.

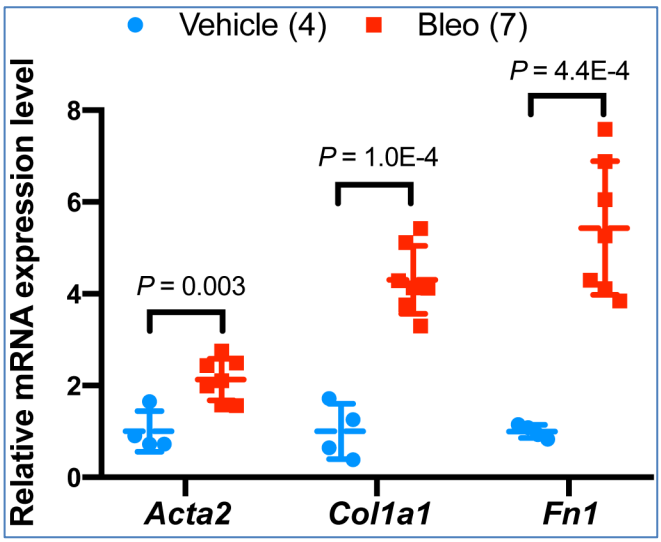

Supplementary Figure 3. Effects of bleomycin on fibroblast activation and ECM deposition in mice lungs. Fold change in the mRNA levels of *Acta2* (α-SMA), *Col1a1* (collagen I) and *Fn1* (fibronectin) in lungs from control (Vehicle) or bleomycin-challenged (Bleo) mice. *Actb* (β-actin)-normalised mRNA levels in control mice lungs were used to set the baseline value at unity. Data are mean ± s.d., with numbers of mice within each group and *P* values indicated. Data were analysed with multiple *t*-test.

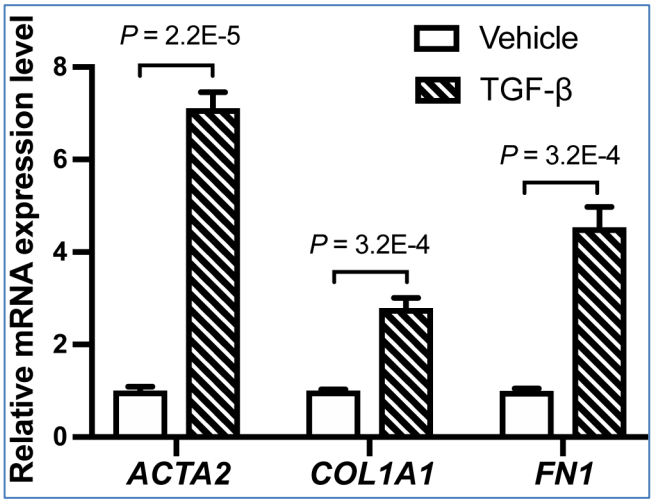

Supplementary Figure 4. Effects of TGF-β on fibroblast activation in HFL1 cells. Fold change in the mRNA levels of *ACTA2* (α-SMA), *COL1A1* (collagen I) and *FN1*(fibronectin) in HFL1 cells with indicated treatments. *ACTB* (β-actin)-normalised mRNA levels in control cells (Vehicle) were used to set the baseline value at unity. Data are mean ± s.d., with *P* values indicated. n = 3 samples each group. Data were analysed with multiple *t*-test.

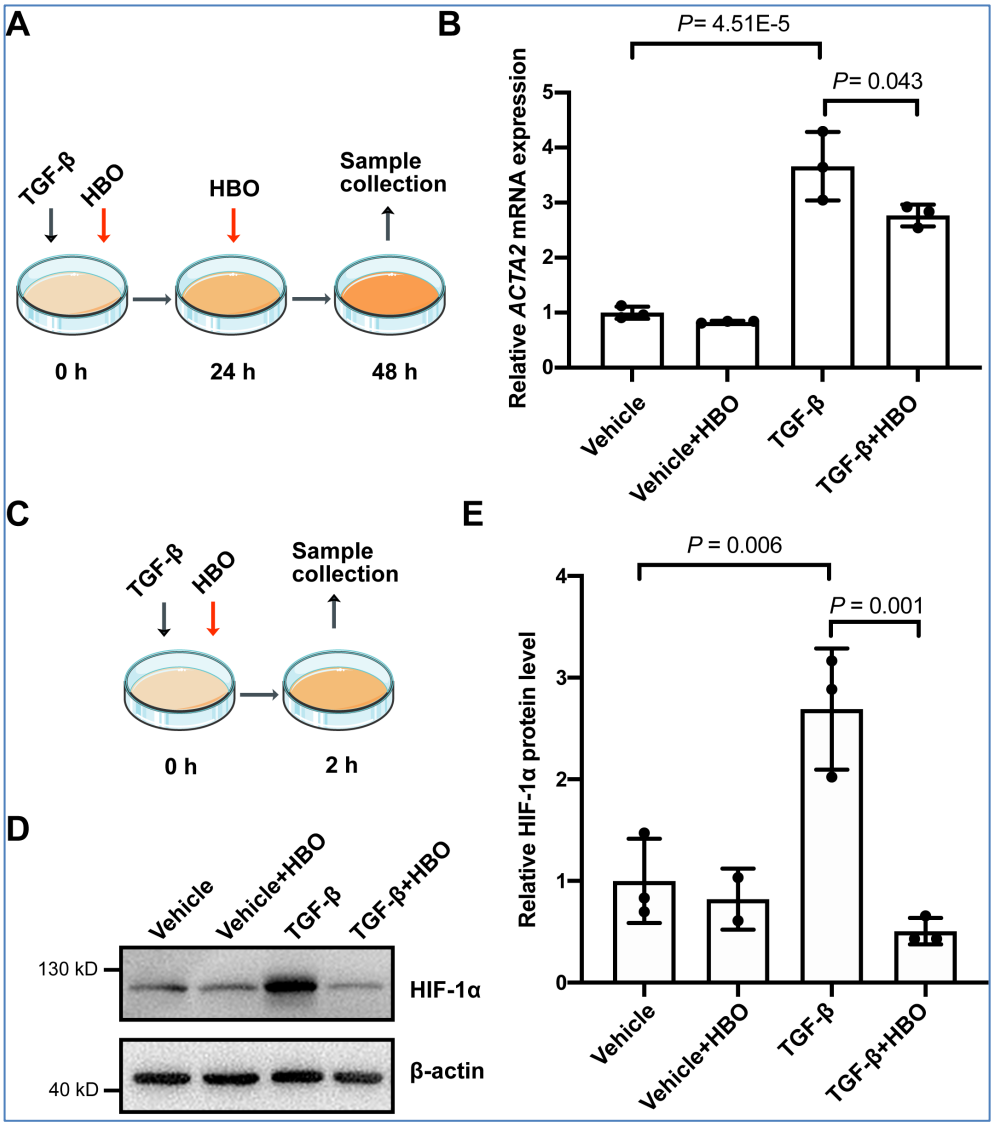

Supplementary Figure 5. Effects of HBO treatment on TGF-β-induced fibroblast differentiation and HIF-1α expression. (A) Schematic diagram of the experimental procedure. In brief, TGF-β (5 ng/mL) was added to HFL1 cells for 48 hours to induce fibroblast activation. At the beginning of TGF-β treatment, HFL1 cells were exposed to 2.5 ATA HBO for 90 minutes immediately. The HBO exposure was repeated for another time at 24 hours post TGF-β treatment. Samples were collected at 48 hours after the beginning of TGF-β treatment. **(B)** Fold change in the mRNA levels of *ACTA2* (α-SMA) in HFL1 cells with indicated treatments. *ACTB* (β-actin)-normalised mRNA levels in control cells (Vehicle) were used to set the baseline value at unity. **(C)** Schematic diagram of the experimental procedure. In brief, HFL1 cells were exposed to 2.5 ATA HBO for 90 minutes right after TGF-β (5 ng/mL) treatment. At the end of HBO exposure, samples were collected immediately. **(D)** Protein expression of HIF-1α in HFL1 cells with indicated treatments. β-actin was used as a loading control. **(E)** Fold change in the protein level of HIF-1α in HFL1 cells with indicated treatments. In the graph, β-actin-normalised protein levels in control cells (Vehicle) were used to set the baseline value at unity. Data in **(B** and **E)** are mean ± s.d., with *P* values indicated. Data were analysed with one-way ANOVA.